

Discovery of a massive SCUBA core with both inflow and outflow motions

Yuefang Wu¹, Ming Zhu², Yue Wei¹, Dandan Xu¹, Qizhou Zhang³ and Jason D. Fiege⁴

ABSTRACT

We report the discovery of a massive SCUBA core with evidence of inflow and outflow motions. This core is detected by SCUBA at both 450 and 850 μm . Barely resolved by the telescope beam at 450 μm , it has a size of $10''$, corresponding to 0.28 pc at a distance of 5.7 kpc. The dust temperature is estimated to be ≤ 29 K, the total mass is $820 M_{\odot}$ and the average density is $1.1 \times 10^6 \text{ cm}^{-3}$ in a region with a radius of $5''$. Follow-up spectral line observations, including HCN (3–2), HCO⁺ (3–2), H¹³CO⁺ (3–2) and C¹⁷O (2–1) reveal a typical blue profile which indicates that this core is collapsing. The CO (3–2) line profile is as broad as 38 km/s, indicating outflow motions in this region. This core is approximately 1.5 pc away from the known HII region G25.4NW, but there are no obvious radio, IRAS, MSX or Spitzer sources associated with it. We suggest that this core is at a very early stage of massive star or cluster formation.

Subject headings: ISM: clouds–ISM: molecules–dust,extinction–ISM: kinematics and dynamics –stars: formation

1. Introduction

Finding massive sources at their earliest stage of star formation is crucial for the study of high mass star formation. Such objects are very difficult to find due to the highly obscured environment and fast evolution of high mass stars. Various surveys were carried out in recent years using molecular lines and dust continuum emission in millimeter and sub-millimeter

¹Astronomy Department, Peking University, Beijing 100871, China, yfwu@bac.pku.edu.cn

²Joint Astronomy Centre/National Research Council of Canada, Herzberg Institute of Astrophysics, 5071 West Saanich Road, Victoria, BC V9E 2E7, Canada

³Harvard-Smithsonian Center for Astrophysics, 60 garden Street, Cambridge, MA 02138, U.S.A

⁴Department of Physics & Astronomy, University of Manitoba, Winnipeg, Manitoba, R3T 2N2, Canada

wavelength bands (Molinari et al. 1996, 2002; Sridharan et al. 2002; Beuther et al. 2002). These surveys, based on IRAS selected samples, have identified a number of precursors of ultracompact (UC) HII regions or high mass protostellar (HMPO) candidates. However, the precursors of UC HII regions or HMPOs usually have $L_{\text{IR}} > 10^3 L_{\odot}$ indicating that the sources are already in a relatively developed stage of star formation. Recently, Garay et al. (2004) reported the discovery of four massive and dense cold cores, which could be the potential sites for future massive star formation.

This letter reports the discovery of a massive cold core using the James Clerk Maxwell Telescope (JCMT). This core was first identified as an ammonia core 18354–0649 (R.A. (1950)=18^h35^m26.5^s, DEC. (1950)= –06°49′32″) during an ammonia survey of massive star formation regions using the MPIfR 100 m telescope at Effelsberg (Wu et al. 2005). Fig.1a shows the NH₃ (1,1) grey scales and (3,3) contours of the IRAS 18355–0650 region overlaid on the VLA 6 cm continuum image (Lester et al. 1985). The center of the NH₃ core is about 80″ away from the IRAS source, and is not associated with any radio continuum emission region. We have made observations using SCUBA at the JCMT as well as a number of molecular lines at sub-millimeter wavelengths. The observational details and data analyses are presented in the following sections.

2. Observations

Dust continuum emission of the ammonia core 18354–0649 was mapped simultaneously at both 850 μm and 450 μm using SCUBA at the JCMT on Sept. 8, 2003. A 64-point jiggle pattern was used, with a chop throw of 150″ along declination (PA=0). Two fields were observed to make a mosaic image covering a 150″ \times 180″ area. Uranus was used for flux calibration, which yielded a flux conversion factor (FCF) of 244 JyV⁻¹ (per beam) with 15% uncertainty at 850 μm and 352 JyV⁻¹ with 30% uncertainty at 450 μm , respectively. Pointing was checked regularly with G34.3. The weather was steadily good, with a CSO 225 GHz $\tau = 0.1$ according to the JCMT water vapor monitor.

A series of molecular lines with different optical depths including the optically thick lines HCN (3–2), HCO⁺ (3–2), CO (3–2) and optically thin lines H¹³CO⁺ (3–2) and C¹⁷O (2–1), were observed toward the detected SCUBA cores in May, 2004 using the Hererodyne receivers A3 and B3 at the JCMT. The receiver temperature, system temperature and telescope beam size were approximately 90 K (200 K), 300–400 K (500–600 K) and 20″ (14″) for A3 (B3). The measured main beam efficiencies η_{mb} were 0.69 for A3 and 0.63 for B3, with 15% uncertainty. A digital autocorrelation spectrometer (DAS) with 250 MHz bandwidth was employed, which provided a velocity resolution of 0.25 km/s. Pointing was checked reg-

ularly using G34.3. Position switching mode was adopted with a reference position of (800", 800"). A test observation indicated that the reference position was free of emission at the relevant frequencies.

HCN (3–2) was sampled at five points along both RA and DEC with 10" spacing centered at the SCUBA core. HCO⁺ (3–2) and C¹⁷O (2–1) were observed in a 3×3 grid. CO(3-2) was observed at 9 points along R.A. and DEC. with 7" spacing. H¹³CO⁺ (3–2) was measured at the center of the SCUBA core. The integration time was 2 minutes each for CO (3-2), 5 minutes each for the HCN (3–2), HCO⁺ (3–2) and C¹⁷O (2–1) lines and 30 minutes for H¹³CO⁺ (3–2).

3. Results and discussion

3.1. The dust core

The SCUBA images at 850 μm and 450 μm of the NH₃ region 18354-0649 are presented as contours in Fig.1. For comparison we have also obtained data from the archives of VLA, IRAS, Spitzer and Midcourse Space Experiment (MSX). The Spitzer IRAC 8 μm and MSX A band, E band (Egan et al. 1998) maps are presented as the background in Fig. 1b, 1c and 1d. The SCUBA dust emission is concentrated in two sub-millimeter cores. The northern core corresponds to the HII region G25.4NW which is detected in the Spitzer and MSX maps as well as in the VLA 6 cm radio continuum map (Lester et al. 1985). The southern core is coincident with the NH₃ peak, which is not associated with any detectable mid-IR and radio continuum emission. This core is therefore named as JCMT 18354–0649S.

The SCUBA maps show that the southern core is more compact than the northern core. At 450 μm , the northern core is resolved, but the southern core is still barely resolved by the 8" beam. Follow up spectral line observations using HCN (3–2), HCO⁺ (3–2) and C¹⁷O (2–1) show that both cores have the same radial velocity V_{LSR} of 95 km s^{–1}, which is quite different from that of the IRAS source IRAS 18355–0650 ($V_{\text{LSR}} = 65$ km s^{–1}). This suggests that these two SCUBA cores are in the same giant molecular cloud, but IRAS 18355–0650 is in a different (foreground) molecular cloud. Using the rotation curve of the Galaxy (e.g. Wouterloot & Brand 1989), the kinetic distance to the SCUBA cores is estimated to be 5.7 or 9.6 kpc depending on whether the source is on the near or far side of the spiral arm. In this letter, we assume a distance of 5.7 kpc, and all the calculations could be easily scaled to a different distance. Our discussion will also focus on the southern core JCMT 18354-0649S.

With a photometric aperture of 25" the total sub-millimeter flux is 6.38 ± 0.96 Jy and

41.8 ± 12.5 Jy at 850 and 450 μm for the core JCMT 18354-0649S.¹ The dust temperature T_d was estimated to be $T_d = 14.4$ K according to a grey body fitting with a dust emissivity index $\beta=2$ ($T_d=25.2$ K if $\beta=1.5$), but it could range from 11.0–29.0 K considering the uncertainty in the SCUBA fluxes and the dust emissivity index. Our result indicates that JCMT 18354-0649S is slightly warmer than those molecular clouds ($T_d < 15\text{K}$) without 100 μm emission (Clark et al. 1991), and is similar to, or warmer than the sourceless cores detected by Garay et al. (2004) (upper limits from 15 to 17 K for $\beta=2$).

The total dust/gas mass of JCMT 18354–0649S is calculated using $M = S_\nu D^2 / \kappa_\nu B_\nu(T_d)$, where S_ν is the flux at frequency ν , D is the distance (5.7 kpc), $B_\nu(T_d)$ is the Planck function, and κ_ν is the dust opacity per unit gas/dust mass. Using the dust opacity $\kappa_{850} = 0.02 \text{ cm}^2\text{g}^{-1}$ and $\kappa_{450} = 0.07 \text{ cm}^2\text{g}^{-1}$ calculated by Ossenkopf & Henning (1994), and assuming a dust temperature T_d of 20 K, a dust to gas ratio of 0.01, we derived a total mass of $M = 910 M_\odot$ and $820 M_\odot$ from the 850 μm and 450 μm flux respectively. The core size is $12'' \times 9''$ which is de-convolved with a $8''$ beam from the measured FWHM value ($14'' \times 12''$). Taking $10''$ as the core diameter and using the mass obtained with the 450 μm at $T_d = 20$ K, the average gas/dust density is $1.1 \times 10^6 \text{ cm}^{-3}$ in the central region with a radius of $5''$, corresponding to 0.14 pc. These results indicate that JCMT 18354–0649S is a cold and high density core.

3.2. Inflow and outflow motions in the southern core

The spectra of HCN (3–2) and HCO^+ (3–2) are shown in Fig. 2a and Fig. 2b respectively. These data indicate that the extent of the dense core traced by HCN (3–2) or HCO^+ (3–2) is within the central $\sim 8''$ after deconvolution, slightly more extended than the dust core seen at SCUBA 450 μm map. This could be an optical depth effect, since HCN or HCO^+ (3–2) are optically thick and would have more contribution from the envelope surrounding the dust core.

The profiles of H^{13}CO^+ (3–2) and C^{17}O (2–1) at the center position are presented in Fig. 2c, together with the HCN (3–2) and HCO^+ (3–2) lines for comparison. The most striking feature is the classical “blue profile”, a line asymmetry with the peak skewed to the blue side in the optically thick HCN/ HCO^+ (3–2) lines, while the optically thin lines H^{13}CO^+ (3–2) and C^{17}O (2–1) both peak at the absorption dip of the optically thick lines. Such feature is a good indication of inflow motions in this massive SCUBA core (Wu & Evans 2003;

¹Using the formula in Seaquist et al.(2004), we estimate that the CO(3-2) line contributes to less than 10% of SCUBA 850 μm fluxes at the peak position. This is within the uncertainty in the 850 μm fluxes and thus no correction was made.

Zhang & Ho 1997; Zhang et al. 1998; Zhou 1999). To further quantify the characteristics of the blue profile, we have calculated the parameter δV , the observed distribution of velocity differences defined by Mardones et al. (1997), derived from optically thick and thin lines, $\delta V = (V_{\text{thick}} - V_{\text{thin}})/\Delta V_{\text{thin}}$. We have two optically thin and two optically thick lines. Thus two peak ratios $T_{\text{A}}^*(\text{B})/T_{\text{A}}^*(\text{R})$ and four δV were derived (Table 1). From Table 1 we can see that the ratios $T_{\text{A}}^*(\text{B})/T_{\text{A}}^*(\text{R})$ from the HCN (3–2) and HCO⁺ (3–2) are greater than 1, and all line pairs have $\delta V < -0.25$, in good agreement with the characteristics of a collapsing core (Mardones et al. 1997).

For a single source, the blue profile can also be produced by rotation. Taking the radius of 8'' and a rotation velocity of 5 km s⁻¹ at this radius, the dynamical mass is estimated to be 1300 M_⊙, which is consistent with that derived from the SCUBA data. However, if the blue profiles in the core JCMT 18354–0649S are caused by rotation, we should also see red profiles. But this was not found in our spectral line maps. In addition, a rotating core should manifest itself with its unique kinematic features such as the rotation pattern in a position-velocity diagram, or the change of intensity ratio between the blue and red peaks across the rotation axis (Ho & Hashick 1986). High resolution interferometer data would be crucial to distinguishing between the rotation and infall scenario for this core. With the single dish data currently available, we did not find any kinematic evidence for rotation.

We have fitted the central spectra of HCN (3–2) and HCO⁺ (3–2) using the analytic model for collapsing clouds provided by Myers et al.(1996). Without taking rotation effect into account, using the equation of radiative transfer and assuming two parallel components of equal temperature and velocity dispersion in a collapsing cloud, the model matches a wide range of line profiles in the candidate infall regions and provides a sensible estimate of V_{in} , the characteristic inward speed of the gas forming the line. Figs.2d and 2e present the plots of the two line fittings respectively. The model parameters defined in Myers et al. (1996) that best fit the two line profiles with the least square method are: $\tau_0 = 9.5$, $V_{\text{in}} = 0.3$ km/s, $T_{\text{k}} = 17.4$ K, $\sigma = 1.8$ km/s for HCN (3–2); and $\tau_0 = 9.0$, $V_{\text{in}} = 0.25$ km/s, $T_{\text{k}} = 16.7$ K, $\sigma = 1$ km/s for HCO⁺ (3–2). The model fitted T_{k} agrees well with the value (17.5 K) that derived from the NH₃ data (Wu et al. 2005). The fitted τ_0 , V_{in} , T_{k} and $\sigma = 1.8$ are much larger than those of low mass cores (Myers et al. 1996), which is consistent with the massive nature of the core. The reasonably good fit suggests that this model can be used for massive cores as well. The “kinematic” mass infall rate, calculated using the formula $dM/dt = 4\pi R_{\text{in}}^2 mnV_{\text{in}}$ (Myers et al. 1996), is estimated to be $3.4 \times 10^{-3} M_{\odot} \text{ yr}^{-1}$. Here a radius of 8'' was adopted for the infall asymmetry zone, and the gas density was assumed as the corresponding mean value of $2.7 \times 10^5 \text{ cm}^{-3}$. For comparison, the “gravitational” rate, defined in Shu (1977), is $1.4 \times 10^{-3} M_{\odot} \text{ yr}^{-1}$ for JCMT 18354–0649S. In the low mass cores, the “kinematic” mass infall rate agrees with the gravitational rate within a factor of 2 (Myers

et al. 1996). In our case, the ratio of these two values is at the higher end, possibly due to the different ISM environment in high mass star forming sites, e.g. higher external pressure.

The HCN (3–2) profile at the center of the sub-millimeter core is remarkably broad. As shown in Fig. 2, the full width of the HCN (3–2) line is 30 km/s. Such a broad wing is a strong indication of outflow motions in the core. It is larger than the total width (about 26 km/s) of the outflow of the high mass protostellar object near IRAS 23385+6053 (Molinari et al. 1998). The extent of outflows of the core JCMT 18354–0649S traced by HCN should be within the central 10'', as the wing is not prominently broad at 10'' offset from the center. We have made follow-up observations at the CO (3-2) transition and the outflow wing is as broad as 38 km/s, from 75 to 113 km/s. From a P-V diagram analysis, the extend of the outflow is $\sim 8''$ (after deconvolve with a 14'' beam). Assuming an incline angle of 60 degree, the derived outflow timescale is 6600 yr. The existence of outflows is consistent with the infall scenario, as outflow is an expected by-product of accretion (e.g. Churchwell 2002). The driving source of outflow could be so deeply embedded that no Spitzer IRAC, MSX or IRAS emissions are detected.

3.3. HMPOs and UCHII regions

SCUBA core JCMT 18354–0649S is a typical cold massive core with more than 800 M_{\odot} . As discussed above, evidence presented in this ~ 0.3 pc region for both inflow and outflow motions suggest that it might be in a hot core phase (Churchwell 2002) — the precursor of UC HII regions (PUCHs), which contains a rapidly accreting massive protostar accompanied by massive bipolar outflows. However, JCMT 18354–0649S is different from a normal hot core. The average temperature is ~ 20 K, and there are no MIR and IRAS sources detected in this region. This core may be at a stage earlier than a normal hot core, and is embedded in large amounts of cold dust.

We calculated the extinction of the core. Taking the neutral hydrogen to $E(B-V)$ ratio as $5.9 \times 10^{21} \text{ cm}^{-2} \text{ mag}^{-1}$ (Bohlin et al. 1978) and the interstellar average value 3.1 for R , we can derive the optical extinction A_V as $3.1 / (5.9 \times 10^{21} / 2) N(\text{H}_2)$. The 4.49 Jy/beam $850 \mu\text{m}$ peak flux density leads to a $N(\text{H}_2) = 6.0 \times 10^{23} \text{ cm}^{-2}$. Therefore the optical extinction A_V is approximately 630 in the core JCMT 18354–0649S, much larger than that in the low mass star forming regions (Visser et al. 2002). So it is not surprising that we could not detect any near-IR and mid-IR emission even if a protostar does exist.

JCMT 18354–0649S is separated from the HII region G25.4NW with a projected distance of 55'' or 1.5 pc (Fig. 1). Both SCUBA cores appear to be distinct isolated objects, but

they have the same radial velocity and seem to be located in the same elongated molecular cloud detected in the ^{13}CO (2–1) map (Lester et al. 1985). The 1.5 pc separation between these two cores is similar to that of the two massive millimeter sources identified by Garay et al. 2004) in an associated filament, and is in agreement with the theoretical predictions of the fragment separations in a filament with density of $3 \times 10^4 \text{ cm}^{-3}$ (Fiege & Pudritz 2000). The fact that massive cores are often found near UC HII regions suggests that the vicinity of UC HII region could be a good place to search for HMPOs.

We are grateful to the JCMT staff for all their assistance with the observations. We also thank an anonymous referee for his valuable comments and suggestions to the draft of this letter. This project was supported by the Grant 10133020, 10128306, 10203003 of NSFC and G1999075405 of NKBRFSF.

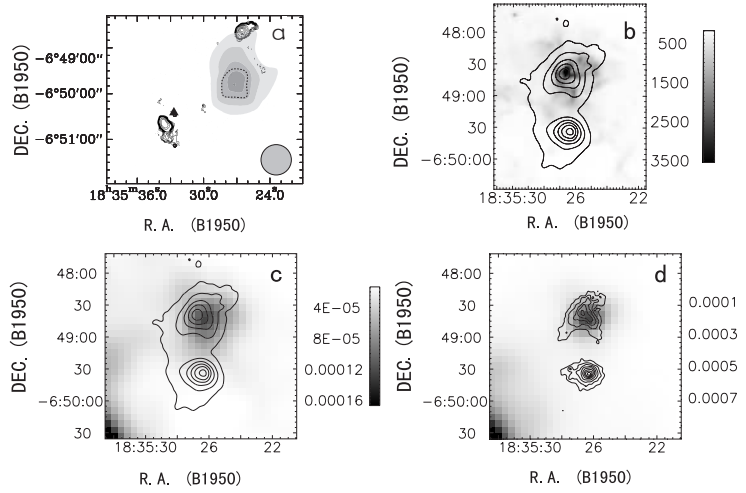


Fig. 1.— a) NH₃ (1,1) (grey scale) and (3,3) (dashed line) overlaid on the VLA 6 cm map (solid line) of G25.4–0.2 (Lester et al. 1985). The northwest and southeast clumpes are the VLA 6 cm compacts of G25.4NW and G25.4SE, respectively (Laster et al. 1985). The solid triangle denotes IRAS 18355-0650, which is the reference position of the NH₃ map. The beam size of the NH₃ observations is indicated in the lower right side of the panel (Wu et al. 2005). b) SCUBA 850 μm contours on IRAC 8 μm band image. The 8 μm flux density scale is in MJy sr⁻¹. Contour levels at 850 μm are from 0.71 (10 σ) to 4.25 by 0.71 Jy/beam. c) SCUBA 850 μm contours on MSX A band image (6.8 – 10.8 μm). Contour levels are the same as in b). d) SCUBA 450 μm contours on MSX E band image (18.2 – 25.1 μm). Contour levels are from 2.9 (5σ) to 17.7 by 2.1 Jy/beam. The MSX flux density is in Wm⁻²sr⁻¹.

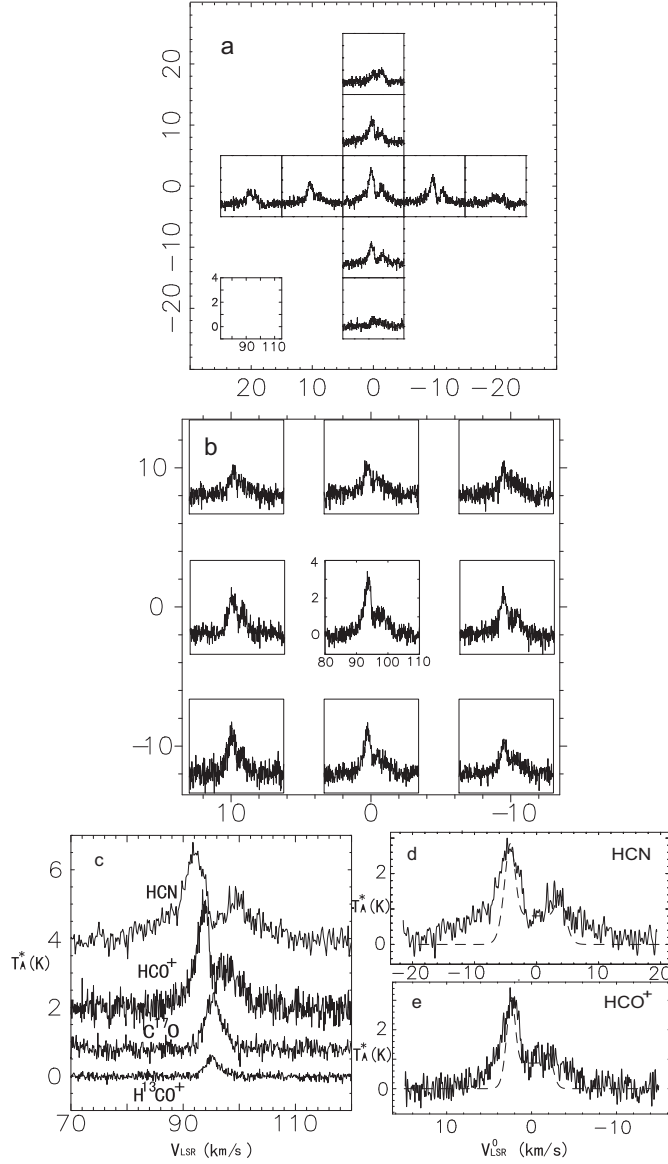


Fig. 2.— Spectral lines of the SCUBA core JCMT 18354–0649S. a) HCN (3–2) grid with 10'' spacing. X and Y axis are the R.A. and DEC. offset in arcsec, respectively. b) HCO⁺ (3–2) grid with 10'' spacing. X and Y axis are the same as a). c) HCN (3–2), HCO⁺ (3–2), C¹⁷O (2–1) and H¹³CO⁺ (3–2) lines at the central position. d) and e) HCN and HCO⁺ (3–2) line (solid line) and model fitting (dashed line) in zero velocity frame (indicated as V_{LSR}^0).

Table 1: Parameters to identify collapse

Thick line		Thin line	
Molecular species	Ratio	Molecular species	δV (km/s)
HCO ⁺ (3–2)	2.11	C ¹⁷ O (2–1)	–0.46
		H ¹³ CO ⁺ (3–2)	–0.48
HCN (3–2)	2.26	C ¹⁷ O (2–1)	–0.50
		H ¹³ CO ⁺ (3–2)	–0.52

REFERENCES

- Beuther, H., Schilke, P., Menten, K. M., Motte, F., Sridharan, T. K. & Wyrowski, F. 2002, *ApJ*, 566, 945
- Bohlin, R. C., Savage, B. D., & Drakes, J. F. 1978, *ApJ*, 224, 132
- Churchwell, E. 2002, *ARA&A*, 40, 27
- Clark, F. O., Laureijs, R. J., & Prusti, T. 1991, *ApJ*, 731m 602
- Egan, M. P., Shipman, R. F., Price, S. D., Carey, S. J. & Clark, F. O. 1998, *ApJ*, 494, L199
- Fiege, J. D., & Pudritz, R. E. 2000, *MNRAS*, 311, 105
- Garay, G., Faundez, S., Mardones, D., Bronfman, L., Chini, R., & Nyman, L. 2004, *ApJ*, 610, 313
- Ho, P. T. P., & Haschick, A. D. 1986, *ApJ*, 304, 501
- Lester, D. F., Dinerstein, H. L., Werner, M. W., Harvey, P. M., Evans, N. J., & Brown, R. L. 1985, *ApJ*, 296, 565
- Mardones, D., Myers, P. C., Tafalla, M., Wilner, D. J., Bachiller, R., & Garay, G. 1997, *ApJ*, 489, 719
- Molinari, S., Testi, L., Rodriguez, L. F., & Zhang, Q. 2002, *ApJ*, 570, 758
- Molinari, S., Testi, L., Brand, J., Cesaroni, R., & Palla, F. 1998, *ApJ*, 505, 139
- Molinari, S., Brand, J., Cesaroni, R. & Palla, F. 1996, *A&A*, 308, 573
- Myers, P. C., Mardones, D., Tafalla, M., Williams, J. P., & Wilner, D. J. 1996, *ApJ*, 465, 133
- Ossenkopf, V. & Henning, T. 1994, *A&A*, 291, 943
- Seaquist, E., Yao, L., Dunne, L., & Cameron, H. 2004, *MNRAS*, 349, 1428
- Shu, F. H. 1977, *ApJ*, 214, 488
- Sridharan, T. K., Beuther, H., Schike, P., Menten, K. M., & Wyrowski, F. 2002, *ApJ*, 566, 931
- Visser, A. E., Richer, J. S. & Chandler, C. J. 2002, *AJ*, 124, 2756

Wouterloot, J. G. A. & Brand, J 1989, A&AS, 80, 149

Wu, Y., & Evans, N. J. 2003, ApJ, 592, L79

Wu, Y., Zhang, Q., Yu, W., Miller, M., Mao, R., Sun, K., & Wang, Y. 2005, submitted to A&A

Zhang, Q., & Ho, P. T. P. 1997, ApJ, 488, 241

Zhang, Q., Ho, P. T. P., & Ohashi, N. 1998, ApJ, 494, 636

Zhou, S. Low mass star formation, ed. W. F. Wall, A. Carraminana, & L. Carrasco, 199